miRNA-mediated regulation of synthetic gene circuits in the green alga *Chlamydomonas reinhardtii*

Francisco J. Navarro & David C. Baulcombe
Department of Plant Sciences, University of Cambridge, Cambridge CB2 3EA, United Kingdom

ABSTRACT
microRNAs (miRNAs), small RNA molecules of 20–24 nts, have many features that make them useful tools for gene expression regulation — small size, flexible design, target predictability and action at a late stage of the gene expression pipeline. In addition, their role in fine-tuning gene expression can be harnessed to increase robustness of synthetic gene networks. In this work we apply a synthetic biology approach to characterize miRNA-mediated gene expression regulation in the unicellular green alga *Chlamydomonas reinhardtii*. This characterization is then used to build tools based on miRNAs, such as synthetic miRNAs, miRNA-responsive 3'UTRs, miRNA decoys and self-regulatory loops. These tools will facilitate the engineering of gene expression for new applications and improved traits in this alga.

KEYWORDS
miRNA, *Chlamydomonas reinhardtii*, gene expression, synthetic gene circuit

Synthetic biology aims to facilitate engineering of living systems using molecular tools that control the expression of endogenous and foreign genes [1]. These tools are often based on the engineering of transcription factor proteins and their binding sites. RNA molecules offer an alternative to protein-based mechanisms as they have the advantage of the relative ease in design, modelling and construction [2,3]. Examples of RNA-based tools of gene expression are riboswitches, aptamers and components of the RNAi silencing pathway, which can be co-opted as sensors, information processors and regulator devices in synthetic gene circuits [4].

RNAi silencing is a highly conserved mechanism that regulates gene expression and defends eukaryotic genomes from viruses and transposons [5]. The trigger of RNA silencing is a double-stranded RNA molecule that is processed into small RNA molecules of 21-24 nts by a RNase III-type nuclease called Dicer [6]. These small RNAs are then associated with proteins of the Piwi/Argonaute family (AGO) to form the RNA-induced silencing complex (RISC). RISC is guided by base pairing of the small RNA to a target RNA that is degraded or translationally suppressed. MicroRNAs (miRNAs) are a species of small RNAs that are derived from imperfect fold-back domains (miRNA precursors) of PolII RNA polymerase transcripts [7]. miRNAs play an important role in regulatory circuits by repressing transcription from leaky promoters, generating thresholds for gene activation and buffering gene expression fluctuations [8]. These features, in addition to their small size and easy targeting design based on sequence complementarity, make miRNAs useful tools in synthetic biology. Artificial miRNAs

(amiRNA) have been widely used for gene silencing both in animals and plants [9,10]. In addition, abundant work on sequence specificity, mode of action and development of miRNA decoy sequences [8,11–13], along with quantitative frameworks [14], have facilitated the use of miRNAs as regulatory devices of gene expression in synthetic gene circuits [15,16].

Chlamydomonas reinhardtii (hereafter referred as "*Chlamydomonas*") is one of few single-celled organisms that possess a functional microRNA pathway [17,18]. This green alga belongs to a lineage that diverged from that of higher plants approximately 1 billion years ago. It has a plant-like chloroplast but animal-like flagellae [19]. A fully sequenced genome [20], extensive transcriptomic data, a large collection of mutants [21], tools for gene expression manipulation [22] and gene editing [23–25] make *Chlamydomonas* a powerful model organism for algal biology and biotechnology. The *Chlamydomonas* miRNA pathway has both plant-like and animal-like features, such as 3' O-methylation, as with plant miRNAs, and overlap with protein coding genes as in animals [17,18,26]. AmiRNAs have been developed in *Chlamydomonas* to knock down endogenous sequences [27,28], and they have been used in reverse genetics experiments and in biotechnological applications [29–31]. However, the use of amiRNAs in synthetic gene circuits requires most extensive analysis of their inhibitory properties and additional tools.

In this work we have expanded the toolkit for gene expression manipulation in *Chlamydomonas* by creating a set of synthetic miRNAs, miRNA-responsive 3'UTRs, miRNA target mimics and miRNA-dependent self-regulatory loops. In addition, we have also established the methodology for the quantitative characterization of miRNA-repression and modulation of the response to miRNA action. These miRNA tools will facilitate the engineering of gene expression for new applications and improved traits.

RESULTS

Design of a miRNA-mediated synthetic gene circuit in *Chlamydomonas*

We designed a simple synthetic circuit to characterize the repressive activity of miRNAs in *Chlamydomonas* (Figure 1A). The circuit has a module in which the expression of a fluorescent protein is linked to the production of a miRNA and a second module in which the mRNA of a second fluorescent protein has the target site for the miRNA of module 1. The first module monitors miRNA abundance *in vivo* and second informs about the level of miRNA repression.

To facilitate the construction of these modules we used Golden Gate cloning [32]. Gene expression regulatory sequences, antibiotic resistance genes, fluorescent reporters and miRNA precursor sequences were codon-optimized for *Chlamydomonas* [33] and "domesticated" for Golden Gate cloning using proposed common syntax [34]. Many of these DNA parts have been added to the *Chlamydomonas* MoClo kit [35]. We describe in the following sections the construction of this gene circuit and characterization of synthetic miRNAs.

A fluorescent protein reporter can be engineered as proxy of miRNA abundance *in vivo* (Module 1)

The accumulation of a miRNA can be monitored by introducing the miRNA precursor sequence inside a fluorescent reporter gene, so that miRNA and mRNA are synthesized from the same RNA molecule [36–38]. This configuration requires the miRNA precursor sequence to be in an intron or in the UTRs of the fluorescent protein gene (Figure 1B). Most endogenous miRNA precursors in *Chlamydomonas* are in fact similarly located within introns or 3'UTRs of protein coding sequences ([26,39]; Supplementary Figure 1A). We therefore created a series of DNA constructs where a miRNA precursor was inserted within the UTRs and intron of a fluorescent protein gene and analyzed the levels of both the miRNA and fluorescence. A similar approach was proposed in the past to facilitate the screen of amiRNA-expressing clones in *Chlamydomonas*[40]. In this previous approach, an amiRNA was cloned between the luciferase gene and the *PSAD* 3'UTR, and some correlation between luciferase activity and amiRNA-dependent repression effect could be observed.

We created an amiRNA using part of the precursor sequence of endogenous miR1157, which has been used before to create amiRNAs [27,40] (Suppl. Figure 1B), except that its sequence was modified to make it compatible with Golden Gate cloning (Supplementary Figure 1C). The miR1157 precursor was suitable for this project because it is a short sequence (137 bp) within the intron of the Cre12.g537671 gene that specifies a single miRNA. To confirm the production of a functional miRNA from this construct we first targeted the *MAA7* gene. *MAA7* is involved in tryptophan metabolism [41] and amiRNA-mediated repression of the gene confers resistance to the metabolic drug 5-fluoroindole (5-FI) [26].

We selected three sites within an mVenus reporter gene to introduce the miRNA precursor sequence: two sites inside an intron in the coding sequence and one site in the 3'UTR (Supplementary Figure 1F). The intron sequence was derived from the second intron of the *RBCS2* that had been scanned using ERISdb [42] to ensure that the miRNA precursor did not disrupt motifs required for splicing. We avoided inserting the miRNA precursor into the 5'UTR because we observed that alteration of this short sequence (46 nts) dramatically reduced the expression of the transgene (see below).

Chlamydomonas wild type strains strongly silence transgenes, posing a major obstacle to obtain high and stable expression of our reporter genes [43,44]. To overcome this challenge, we used the UVM11 strain for all of the subsequent experiments [45]. This mutant strain supports high and robust transgene expression which is not silenced over time [46]. However, it is not known whether the mutation(s) responsible for the high transgene expression affects the miRNA pathway. We investigated this point by analyzing cleavage products of endogenous miRNAs (Supplementary Figure 2A) and testing the functionality of an amiRNA against the *MAA7* gene (Supplementary Figure 2B). Our results showed that the miRNA pathway is functional in the UVM11 strain. Therefore, we used this strain for the construction of miRNA-based gene circuits.

The control module 1 construct had mVenus genes without a miRNA (mVenus_PSAD or mVenus_RBCS depending on the 3'UTR) fused to the paromomycin resistance cassette. The transformants (mVenus_PSAD, mVenus_RBCS) expressed different levels of mVenus due to the random integration of the construct and chromatin context-dependent expression (Figure 1C; Supplementary Figure 2C). These

levels of mVenus fluorescence were much higher than the autofluorescence of the UVM11 strain (Figure 1C, “backgr.”) or of clones transformed only with the antibiotic resistance cassette (Figure 1C, “neg.control”; Supplementary Figure 2C).

The miRNA precursor sequence in either of the intronic sites did not interfere significantly with the expression of the mVenus gene (“mVenus_PSAD +miR intron site 1 and 2”, Figure 1C). In contrast, the introduction of the miRNA precursor in the 3’UTR (mVenus_RBCS +miR ter. site 3) prevented mVenus expression, most probably due the truncation of the mRNA by the action of Dicer. We therefore selected the reporter system with intronic miRNA precursor in site 2 to test the relationship of miRNA abundance and fluorescence.

Northern blot of the amiRNA in different clones revealed a linear correlation between the mVenus fluorescence and miRNA abundance (Figure 1D, 1E) at low and intermediate levels (Figure 1E). The miRNA produced from our reporter system was functional, as evidenced by the fact that clones with high mVenus fluorescence were resistant to 5-FI, indicating repression of the *MAA7* gene (Figure 1F). In contrast, clones transformed with the control construct (the mVenus gene lacking the intronic miRNA precursor) were unable to grow on media containing 5-FI. In conclusion, the engineering of an intronic miRNA precursor inside the mVenus gene allows the use of fluorescence as a proxy for the amount of miRNA inside the cell.

Construction of a reporter system to measure miRNA-mediated gene repression activity of a miRNA (Module 2)

For the construction of module 2 of the miRNA-mediated synthetic gene circuit, we used a second fluorescent protein, mCherry, as part of a two-color reporter system to measure the repressive activity of a miRNA. The emission spectra of mCherry and mVenus are non-overlapping, allowing simultaneous quantification of both fluorescent signals *in vivo*.

To optimize the amiRNA targeting we introduced the 21-nt amiRNA target sequence at three different locations: in the 5'UTR right upstream of the Start codon (site A), 4-nt downstream the Stop codon (site B), and 119-nts upstream of the polyadenylation site (site C) (Figure 2A). Clones expressed high levels of mCherry fluorescence when the 21-nt miRNA target site was introduced into both sites of the 3’UTR and low levels when it was in the 5’UTR (Supplementary Figure 3), likely due to disruption of motifs important for protein translation.

We then transformed a single line with high levels of mCherry with mVenus constructs fused to a paromomycin resistance cassette. Double transgenic lines with the paromomycin resistance had varying levels of mVenus and mCherry (Figure 2B) depending on the amiRNA target site and whether mVenus included the intronic miRNA (Figure 2B, “mVenus (+intr. miRNA)” vs “mVenus”). The mCherry fluorescence was reduced by the amiRNA when the miRNA recognition site was in the 5’UTR (site A, Figure 2B) or close to the polyadenylation site in the 3’UTR (site C, Figure 2B). There was no reduction when the target site was introduced close to the stop codon (site B) (Figure 2B). We chose site C for our further analysis because there was significant amiRNA repression against a background of high level of mCherry fluorescence.

Generation of synthetic miRNAs and target 3'UTRs

We next proceeded to design "synthetic miRNAs" (artificial miRNAs with target sequences not present in the *Chlamydomonas* genome) for incorporation into this two module system using the MicroRNA Designer tool of the WMD3 website [47]. The algorithm was fed with a scrambled sequence of a randomly selected *Chlamydomonas* gene as target sequence and the miRNA sequences generated were filtered based on the following criteria: predicted high efficiency and specificity, GC content within the range of endogenous miRNAs, absence of ATG/CAT triplets, and absence of the *Bpi*I/*Bsa*I recognition sites that are used for the Golden Gate cloning. In addition the miRNA sequences had to have a uridine residue at the first position of the 5' end, a feature that is observed in most endogenous miRNAs in *Chlamydomonas* [17,18] and there should be no potential "off targets" with full sequence complementarity in the *Chlamydomonas* genome. We selected seven of these sequences to test their repressive activity (Figure 3).

We introduced 21-nt sequence with perfect complementarity to each of the seven synthetic miRNAs into site C (Figure 2) of the mCherry reporter gene and then re-transformed strains with high levels of mCherry fluorescence with mVenus cassettes with synthetic miRNAs at intronic site 2 (Figure 3A, 3B). The mVenus cassette lacking the miRNA precursor was the control. All seven synthetic miRNAs repressed the mCherry by varying levels between 66 and 93% (Figure 3C). Our two-module system is, therefore, a functional framework for characterization of synthetic miRNAs in *Chlamydomonas*.

Characterization of the repressive activity of a synthetic miRNA

We selected the synthetic miRNA miR1 as an example to characterize the repressive activity of synthetic miRNAs. Clones displaying varying levels of mVenus showed a high degree of anti-correlation with mCherry, only when the mVenus gene had the intronic miRNA (Figure 4A). mCherry fluorescence plateaued at low-intermediate level of mVenus (Figure 4B), indicating that the mCherry mRNA was hypersensitive to miR1 levels.

We also characterized miR1-dependent repression at molecular level by Northern blotting (Figure 4C). The mVenus fluorescence, mVenus mRNA and miR1 levels correlated well (Figure 4A) and, as expected, the levels of the mCherry mRNA reduced as the levels of mVenus mRNA and miR1 increased. The decrease in mCherry mRNA was associated with the appearance of two bands that, based on their size, could correspond to full length and miR1-dependent cleaved transcripts.

Consistent with this interpretation we detected an RT-PCR product from 3'UTR of the mCherry gene by 5'RACE (Figure 4D) in clones expressing the mVenus gene with the intronic miR1 precursor (Figure 4D, "+intronic miRNA") but not from clones with the mVenus gene lacking the miRNA (Figure 4D, "mVenus"). The 5' end of the RT-PCR was complementary to positions 10 and 11 of miR1 (Figure 4E), confirming the specificity of the miRNA-dependent cleavage of mCherry mRNA and that mCherry silencing by miR1 occurs by RNA degradation instead of translational repression.

We extended our characterization to single cell level by using fluorescence microscopy. Cultures of double transgenic lines expressing mCherry and mVenus with intronic miR1 precursor (Figure 4F top panels), or without miRNA (Figure 4F, bottom panels) were mixed with cells expressing only the mCherry reporter in order to compare mCherry fluorescent levels. As expected, cells displaying mVenus fluorescence in the transgenic line that expressed miR1 had reduced levels of mCherry fluorescence. In contrast, mCherry fluorescence was not reduced in mVenus positive cells that did not harbor intronic miR1 (bottom panel). In conclusion, our characterization shows specific and efficient silencing by synthetic miRNAs at population and single cell level.

Modulation of the miRNA repressive activity

The silencing activity of a miRNA relies on sequence complementarity to its target [8,11] and alteration of this complementarity can be used as a way to modulate the response of a target mRNA. Yamasaki et al. previously showed that complementarity to a *Chlamydomonas* miRNA seed region was sufficient to induce moderate repression [48]. We further analyzed the effects of sequence complementarity with our two-module system. In order to change the repression activity of the synthetic miRNAs, we mutated the two nucleotides that flank the miR1-RISC cleavage site on mCherry transcript (sites opposite to positions 10' and 11' of miR1) (Figure 5A) and transformed with an mVenus construct carrying the intronic miR1 precursor. As control, we also transformed a line expressing mCherry carrying a target site with perfect complementarity to miR1. The 2-nt mismatch on miR1 target site reduced silencing of mCherry compared to the control (Figure 5A): the control mCherry construct was silenced at high mVenus levels down to 15% of the initial value whereas, with the mutant target and similar mVenus levels, the mCherry fluorescence reduced down to 40%. In addition, there was a more gradual gradient of silencing of mCherry with the mismatched target (Figure 5A).

mCherry mRNA levels, determined by RT-qPCR, correlated with fluorescence (Figure 5B) indicating that, even in the absence of perfect complementarity, miR1 triggers silencing of mCherry by RNA degradation. Consistent with this interpretation the miR1-dependent cleavage products of mCherry mRNAs were present for both types of target site, although at lower levels with 2nt-mismatch (Figure 5C-E).

Altogether, these results show that the introduction of mismatches at miRNA target site modulates the miRNA-dependent silencing and provides a method to obtain a close to linear relationship between the miRNA and target levels.

A miRNA decoy partially inactivates a synthetic miRNA

As well as modulating the activity of a miRNA, it would be interesting to develop tools that inactivate miRNAs in *Chlamydomonas* such as miRNA decoys (for reviews [49,50]). These are RNA molecules carrying sequences with high complementarity to a miRNA that specifically sequester and/or trigger the degradation of the miRNA, resulting in the de-repression of its targets.

To assess the functionality of miRNA decoys in *Chlamydomonas*, we designed a miRNA decoy in which one (RNA decoy 1X) or two (RNA decoy 2X) 24-nt sequences with perfect complementarity to miR1, except for a 3-nt bulge at the RISC cleavage site were

introduced into the 3'UTR of a mVenus gene (Figure 6A, Supplementary Figure 4A). It has been shown before that miRNA decoys embedded into the 3'UTR of β-glucorinadase (GUS) are effective at inactivating plant miRNAs [51,52]. In our case, the 3'UTR was derived from the PSAD gene, and a 48-nt linker sequence identical to the one used in [53] was inserted in between the two miR1 mimic sites. A construct without mimic sites was used as control.

The miRNA decoys were fused to a zeocin resistance cassette and transformed into one of the double transgenic lines described in the previous section (Figure 6B) in which mCherry was silenced by miR1 from an mVenus gene. The miRNA target in mCherry carried a miR1 target site with a 2nt-mismatch (Figure 5E).

Transformants carrying either RNA decoy 1X and 2X had higher mCherry fluorescence than transformants with the control mVenus construct (Figure 6C), and lower mCherry fluorescence than transformants lacking miR1. These results therefore suggest that our miRNA decoy constructs triggered partial de-repression of the mCherry gene. This de-repression of mCherry was not potentiated by the presence of a second mimic site in the miRNA decoy. The derepression effect of the miRNA decoy was less in cells in which the miRNA target site was perfectly complementary to miR1 (Supplementary Figure 4B).

From these results we conclude that miRNA inactivation by miRNA decoys is possible in *Chlamydomonas* and can be incorporated into the design of miRNA-based synthetic gene circuits. However, efficient miRNA inactivation will require additional optimization of the miRNA decoy design and expression, and it will be influenced by the degree of sequence complementarity between the miRNA and its target RNA (Supplementary Figure 4B).

Construction of self-regulatory loops using intronic miRNAs.

miRNAs can be engineered into feed-forward loops, which may buffer gene expression noise and adaptation to stimuli [54,55]. To explore this possibility in *Chlamydomonas* we used the elements characterized above to construct an intronic miRNA self-regulatory loop (iMSL), consisting of an intronic miRNA that silences the mRNAs derived from the same molecule as the miRNA (Figure 7A). This simple circuit has the potential of extending auto-regulatory properties to genes which are not transcriptional factors.

To create an iMSL, we fused the coding sequence of the mVenus gene, harboring an intronic miRNA precursor, with the PSAD-derived 3'UTRs described earlier. These 3'UTRs carried a target site for the intronic miRNA. We tested two different 3'UTRs, one carrying a target site with high complementarity to the intronic miRNA (construct 3), and a second with two extra mismatches to the miRNA at positions 8' and 9' (construct 4) (Figure 7B). These mismatches reduced the silencing effect of the miRNA when this was expressed from a different gene (Supplementary Figure 5A), similarly to what was described in a previous section. A construct lacking the intronic miRNA precursor and target sequence (construct 1), and another construct with the intronic miRNA precursor but without the target sequence (construct 2), were used as controls. In each instance,

the mVenus gene was fused to the paromomycin resistant cassette for the isolation of transformants.

mVenus fluorescence of individual clones from each transformation is shown in the boxplot in Figure 7C. Transformation with control constructs 1 and 2 produced transformants with a broad range of fluorescence intensities whereas, with construct 3, where an iMSL was implemented, the transformants had very low levels of fluorescence due to self-silencing. The presence of mismatches into the miRNA target sequence (construct 4) partially recovered the mVenus fluorescence levels, most likely due to reduced self-silencing. These results confirm that miRNA-mediated iMSL are functional in *Chlamydomonas* and can be engineered.

Mathematical modeling predicts that gene expression variability would be buffered by an iMSL in which the miRNA has low/intermediate repressive activity [56]. To test this possibility, we analyzed cell-to-cell variability in mVenus fluorescence in clones carrying the constructs described in the previous section. Quantification of single cell fluorescence was performed using flow cytometry [57]. As an example of an iMSL with intermediate repressive activity we used construct 4. In addition, to distinguish the effect of the self-regulation versus miRNA repression, we included a control construct similar to construct 4 except for the fact that the miRNA was not linked to the mVenus mRNA (Figure 7B).

Figure 7D shows that the CV^2, as a measurement of variability, changed with the average level of expression, and it increased as expression decreased. Clones carrying the iMSL (construct 4) had less variability than the controls (constructs 1 and 2), especially at intermediate and low levels of average mVenus expression. However, there was a similar reduction in cell-to-cell variability when the miRNA was produced independently of the mVenus mRNA (control construct). These results suggest that miRNA repression is enough to confer certain buffering against variability but that the presence of an iMSL does not add extra buffering capacity, at least under the conditions assayed.

DISCUSSION

In this work we have constructed a two-module miRNA system with applications in synthetic biology in *Chlamydomonas*. The most obvious application is in the design of a negative switch for gene silencing. We show how the negative miRNA regulator can be most usefully integrated into an intron, and how the expression level of a reporter construct encoded in the adjacent exons can be used to indicate the relative level of the miRNA (Figure 1). In the present work, this design was under a constitutive promoter but, in principle, a similar design can be used under inducible or regulated promoters.

It is likely that miRNAs in nature are fine tuners rather than two-state on/off regulators of gene expression [52,58]. Such fine-tuning would also be useful in synthetic biology. We were able to confirm this role of miRNAs in *Chlamydomonas* by varying miRNA levels and by modifying the complementarity between the miRNA and target sequences (Figures 4 and 5). It is likely, however, that robust and stable intermediate levels of gene silencing are more easily achieved by changing sequence

complementarity rather than through modulation of the miRNA abundance. We showed that perfect complementarity between the target site and the miRNA showed a non-linear relationship between the miRNA levels and the degree of target silencing (Figure 4 and 5). With the mismatched target-miRNA (Figure 5), however, this relationship was more linear, facilitating the isolation of intermediate levels of expression. A similar effect has been described for an animal miRNA when affinity for its target was reduced[14]. It is likely that this result could be extended to other miRNA sequences.

A third potential application of miRNAs is to reduce noise in the expression of synthetic gene modules [59]. Our original idea, supported by mathematical modeling [56], was that a single component system with self-regulatory capacity by implementation of a cis-acting miRNA would achieve noise reduction (Figure 7). Although this was the case, there was, however, a similar noise reduction by action of a trans-acting miRNA, suggesting the existence of feedback between miRNA-mediated regulation and the other mechanisms affecting RNA accumulation. Schmiedel et al. showed that reduction of the intrinsic noise of protein expression is a generic property of animal miRNAs [60]. It is possible that the noise buffering effect that we have measured could be attributed to this generic property.

We have pointed out elsewhere that the miRNA system of *Chlamydomonas* is atypical of both land plants and animals [26,39]. Our finding that mismatched miRNAs mediate target RNA cleavage (Figure 5D and E) provides further support for this idea. The atypical nature of the *Chlamydomonas* miRNA system is also reflected in the finding that miRNA decoys are only partially effective at blocking the action of a miRNA.

Several possibilities can account for the lack of efficiency of miRNA decoys in *Chlamydomonas*. One possibility is that the machinery responsible for miRNA degradation upon binding the decoy molecule is missing in *Chlamydomonas*. Little is known about the algal miRNA degradation pathway, and no functional homologs of *SND1* and *SND2*, which are involved in decoy-triggered miRNA degradation in *Arabidopsis* [53], have been identified.

Another possibility is that a higher accumulation of the miRNA decoy relative to the miRNA is required to obtain effective degradation of the target miRNA. We tried to maximize expression of the miRNA decoy by expressing the construct under a strong promoter (*PSAD*) and by linking it to the zeocine selection marker, previously shown to promote high levels of expression of recombinant sequences [61]. However, as our miRNA decoy was part of a mRNA molecule, its degradation might be faster than the miRNA itself and prevent accumulation.

Finally, it is also possible that the miRNA and our miRNA decoy construct accumulate in different subcellular compartments in *Chlamydomonas*. As our miRNA decoy molecule is a mRNA, we expect that it most likely accumulates in the cytoplasm associated with ribosomes. If, on the other hand, the RISC complex is predominantly in other cytoplasmic sub-compartments or in the nucleus, this might prevent the action of the decoy. Being the case, incorporating decoy sequences onto molecules that do not associate with polysomes, such as nuclear RNAs or long non-coding RNAs (Franco-Zorrilla et al., 2007) could result in higher efficiency of the decoy. Alternative designs incorporating the decoy sequences into RNA molecules more resistant to degradation,

such as circular RNAs and TuD hairpins [62], could be implemented to increase the accumulation of the miRNA decoy molecule.

The tools and methodology described in this work will be useful to investigate these possibilities and to guide future efforts for the engineering of gene expression in this alga although it is clear that each miRNA circuit will need to be optimized and tested for off-target effects.

There is abundant work on miRNA-based regulation in animal cells, using reporter systems similar to the ones described in our work. Animal miRNAs have also been used to engineer synthetic circuits with complex behaviors. This level of characterization and application is missing in plants, and the present work can be used as a proof-of-principle for further miRNA-based manipulation of gene expression in the alga and higher plants. Our work establishes the basic tools and design for this aim. In addition, some of the findings of the current work may prompt further investigation in animal systems, or inspire new circuit designs to, for example, reduce cell-to-cell variability of a gene under the repression of a miRNA, independently of the presence of a self-mediated loops. , and another is the use of synthetic miRNAs, which avoid using endogenous miRNAs.

METHODS

Strains, growth conditions and transformation

The *Chlamydomonas* cell-wall deficient strain UVM11 strain, kindly provided by Dr Ralph Bock (Max Planck Institute of Molecular Plant Physiology, Germany), was used in this work (Supplementary Table S1). This strain was originally isolated in a screen for mutant strains which expressed high levels of a transgene [45]. In some experiments the strain CC-1883, obtained from the *Chlamydomonas* Resource Centre was used (Supplementary Table S1). Liquid or solid 2-amino-2-(hydroxymethyl)- 1,3-propanediol (TRIS)-acetate-phosphate (TAP) media was used as growing media [63], and cultures were incubated at 25°C under continuous illumination (125 µE m^{-1} s^{-1}). To test suppression of the *MAA7* gene, TAP media was supplemented with 10 µM of the metabolic drug 5-fluoroindole (5-Fl, Merck), from a stock solution of 1 mM prepared in DMSO. For selection of transformants, TAP media was supplemented with 15 µg/ml paromomycin, hygromycin or zeocin.

For transformation, 50 ml cultures were grown up to approximately $5x10^6$ cells/ml, spun down and resuspended in 0.9 ml TAP. Cells were mixed with 200-500 ng of a linear DNA fragment that carries the indicated DNA cassette excised from the plasmid backbone and further purified from an agarose gel. The mix was split into three tubes containing 0.3 ml of 400-600 nm diameter glass beads, and shaken on a vortex mixer at max speed for 15 sec. The cell suspension was then transferred onto solid TAP containing the appropriate antibiotic. Plates were incubated in dark for 2 days, and then under continuous light until the appearance of colonies. Colonies were picked and streaked out onto fresh TAP plates containing antibiotics.

Plasmid construction

Plasmids used in this work were constructed using a modular strategy based on Golden Gate cloning and following the syntax proposed previously [34]. Backbones described in [64] were used, and *Chlamydomonas* specific level zero DNA parts were created by site-directed mutagenesis or gene synthesis. Conditions for the one-pot digestion-ligation reaction were 37°C for 20 sec, 26 cycles of 37°C for 3 min-16°C for 4 min, and finally 5 min at 50°C and 5 min at 80°C. Many of the DNA parts used in this work have been added to the Chlamy MoClo kit [35] or have counterparts in the kit.

miRNA precursors encoded inside the intron sequence of the mVenus gene were constructed by Golden Gate (Supplementary Figure 6). The miRNA precursor sequence was assembled using five short dsDNA molecules of 48 to 74 bp, each formed by two annealed complementary oligonucleotides. Each of the dsDNA fragments carried *BpiI* sites on both ends that generated different overhangs upon digestion, allowing assembly and directional cloning into recipient plasmid pFJN61. The one-pot digestion-ligation reaction consisted in 0.045 pmol of plasmid pFJN61, 0.175 pmol of each dsDNA fragment, 1X NEB T4 DNA ligase buffer, 0.1 mg/ml of BSA, 5U of BpiI (Thermo) and 200U of NEB T4 DNA ligase, in a 15 µl volume reaction. The reaction was incubated as described above. dsDNA fragments were annealed by incubating 500 pmol of each oligonucleotide in 10 mM Tris-HCl pH 8.0, 1 mM EDTA, 0.1 M NaCl, at 95°C for 4 min, and then let to cool down to room temperature for 10 min. Once the miRNA precursor sequence was incorporated into the intron, the assembly of the remaining mVenus gene was performed as described in [35] by Golden Gate cloning. The level 2 acceptor plasmid of choice was pFPC2, derived from pAGM4723 [65]. The pFPC2 plasmid lacks sequences for *Agrobacterium* T-DNA integration, and has symmetrical *BsaI* sites to separate the multigene cassette from the backbone sequence. After *BsaI* digestion, the multigene cassette was extracted from gel and used for transforming *Chlamydomonas* as described above.

To incorporate miRNA target sequences into the *PSAD* 3'UTR, we employed the NEB Q5® site-directed mutagenesis kit, using primers described in Supplementary Figure 6D. The modified 3'UTRs were sequenced and assembled into transcriptional units and multigene cassettes as described in [35].

RNA extraction

RNA isolation was carried out as previously described [17]. A detailed protocol can be found at http://www.plantsci.cam.ac.uk/research/davidbaulcombe /methods/downloads/smallrna.pdf/view. We did the following modifications on the protocol: RNA was extracted from live cells after centrifuging the culture, without prior freezing; PureZol (Biorad) was used instead of Trizol and volumes were scaled down to perform extraction in 2 ml tubes. RNA quality was assessed in gel and quantified in Nanodrop (ThermoFisher scientific). RNA was stored at -80°C.

Northern blots and qPCR

Small RNA detection by Northern blot was performed as previously described in [17] (http://www.plantsci.cam.ac.uk/research/davidbaulcombe/methods/downloads/smallrna.pdf/view) (Supplementary Methods). Probe sequences are indicated in Supplementary Table S2.

cDNA for relative quantification of gene expression by qPCR was made from 5 µg total RNA using SuperScript IV Reverse Transcriptase (RT) (ThermoScientific) and primed with oligo dTs. 5 µg of total RNA was retro-transcribed with 200 U of RT at 55°C for 1 h. RT was inactivated at 80°C for 10 min. Contaminating DNA in the RNA sample was removed with 2 U of TurboDNase (ThermoScientific) for 20 µg of total RNA, incubating at 37°C for 30 min. cDNA was diluted 1:20 and 4 µl were used in a 25 µl PCR reaction containing 0.3 µM of each primer, 2.5 U of Taq polymerase (PCRbio), 4% (v/v) DMSO, 5 mM dNTPs and 1X SYBR Green (ThermoScientific). A control qPCR reaction from each sample treated with DNase but no RT was carried out to assess potential genomic DNA contamination. 1:5, 1:10, 1:50, 1:100 dilutions of the sample expecting to have higher levels of expression of the desired gene were used to assess for inhibition of the qPCR and for quantification. Oligos used for qPCR are indicated in Supplementary Table S2. PCR conditions were: an initial denaturation step at 95°C for 2 min, and 40 cycles of 95°C 10 seconds, 57.4°C for 10 seconds and 72°C for 10 seconds. Melting curve at the end of the run and agarose electrophoresis confirmed single and specific product of the PCR.

miRNA cleavage site determination by 5'RACE

miRNA cleavage site determination was performed as previously described [66]. Briefly, 10 µg of total RNA was ligated with an RNA oligo (5'-CGACUGGAGCACGAGGACACUGACAUGGACUGAAGGAGUAGAAA-3') by using T4 RNA ligase for 1h at 37°C. RNA was purified with phenol:chloroform and precipitated with ethanol and sodium acetate. The precipitated RNA was retrotranscribed into cDNA with SuperScript IV reverse transcriptase (ThermoScientific) and random hexamers by following manufacturers recommendations. Then, 2 µl of the generated cDNA were used as template of a PCR using primer 456 and a gene specific primer (Supplementary Table S2). Finally 2 µl of this PCR was used as a template of a second PCR with primer 457 and a nested gene-specific primer. The PCR product was resolved in a 2% (w/v) agarose gel and those DNA fragments with the expected electrophoretic mobility were isolated from the gel and cloned into pGEM-T easy (Promega) for further Sanger sequencing.

Fluorescence measurements in plate reader

Fluorescence measurement from live cells was made in a FLUOstar Omega microplate reader (BMG Labtech). Data was analyzed in R (Supplementary Methods).

Flow cytometry

Cultures were grown to 1-2x10^6 cell/ml cell density, and fluorescent signals were acquired in a BD FACScan (Cytek modified). mVenus- and mCherry-derived fluorescence signals were determined by using 488 nm and 561 nm lasers, respectively, and the

following fluorescence parameters: FL-1 (530/30 nm) for mVenus and 615/25 nm for mCherry. Chlorophyll was detected with the 488 nm laser and FL-3 (695/40 nm). Flow cytometry data was analyzed using FlowJo software (FlowJo). Flow cytometry data were exported from FlowJo using the option "CSV-scale", and processed in R (Supplementary Methods).

Fluorescence microscopy

Live cells were imaged using a DMI6000B Leica inverted microscope, equipped with a 63X PLANAPO oil immersion objective (1.4 NA). mVenus and mCherry fluorescent filters were 490-510/515/520-550 nm and 540-552/560/567-643 nm (Ex./DC/Em.), respectively. Samples were prepared in TAP media using 8-well glass bottom µ-slides (Ibidi), covered with poly-L-lysine (Sigma). Images were acquired using LAS X software, and analyzed using ImageJ software.

ASSOCIATED CONTENT

Supporting Information

Additional Figures as described in the text and Supplementary Methods (pdf)

Funding

This work was supported by OpenPlant, which receives its funding from the Biotechnology and Biological Sciences Research Council (BBSRC) and the Engineering and Physical Sciences Research Council (EPSRC). D.C.B. is supported as the Royal Society Edward Penley Abraham Research Professor.

Acknowledgements

We would like to thank Ralph Bock (Max Planck Institute for Molecular Plant Physiology, Germany) for the UVM11 strain, Alison Smith and Jim Haseloff (University of Cambridge) for reagents and support, and Adrian Valli and Bruno Martins for critical reading of the manuscript.

References

(1) Kitney, R. (2009) Synthetic biology. *Synth. Biol. scope, Appl. Implic.* London.
(2) McKeague, M., Wong, R. S., and Smolke, C. D. (2016) Opportunities in the design and application of RNA for gene expression control. *Nucleic Acids Res. 44*, 2987–2999.
(3) Benenson, Y. (2012) Synthetic biology with RNA: Progress report. *Curr. Opin. Chem. Biol. 16*, 278–284.

(4) Liang, J. C., Bloom, R. J., and Smolke, C. D. (2011) Engineering Biological Systems with Synthetic RNA Molecules. *Mol. Cell 43*, 915–926.
(5) Baulcombe, D. (2004) RNA silencing in plants. *Nature 431*, 356–363.
(6) Carthew, R. W., and Sontheimer, E. J. (2009) Origins and Mechanisms of miRNAs and siRNAs. *Cell 136*, 642–655.
(7) Ghildiyal, M., and Zamore, P. D. (2009) Small silencing RNAs: an expanding universe. *Nat Rev Genet 10*, 94–108.
(8) Bartel, D. P. (2009) MicroRNAs: Target Recognition and Regulatory Functions. *Cell 136*, 215–233.
(9) Zeng, Y., Wagner, E. J., and Cullen, B. R. (2002) Both natural and designed micro RNAs can inhibit the expression of cognate mRNAs when expressed in human cells. *Mol. Cell 9*, 1327–1333.
(10) Schwab, R., Ossowski, S., Riester, M., Warthmann, N., and Weigel, D. (2006) Highly Specific Gene Silencing by Artificial MicroRNAs in Arabidopsis. *Plant Cell 18*, 1121–1133.
(11) Voinnet, O. (2009) Origin, Biogenesis, and Activity of Plant MicroRNAs. *Cell 136*, 669–687.
(12) Axtell, M. J., Westholm, J. O., and Lai, E. C. (2011) Vive la différence: biogenesis and evolution of microRNAs in plants and animals. *Genome Biol. 12*, 221.
(13) Steinkraus, B. R., Toegel, M., and Fulga, T. A. (2016) Tiny giants of gene regulation: Experimental strategies for microRNA functional studies. *Wiley Interdiscip. Rev. Dev. Biol. 5*, 311–362.
(14) Bloom, R. J., Winkler, S. M., and Smolke, C. D. (2014) A quantitative framework for the forward design of synthetic miRNA circuits. *Nat. Methods 11*, 1147–1153.
(15) Xie, Z., Wroblewska, L., Prochazka, L., Weiss, R., and Benenson, Y. (2011) Multi-Input RNAi-Based Logic Circuit for Identification of Specific Cancer Cells. *Science 333*, 1307–1311.
(16) Nissim, L., Wu, M.-R., Pery, E., Binder-Nissim, A., Suzuki, H. I., Stupp, D., Wehrspaun, C., Tabach, Y., Sharp, P. A., and Lu, T. K. (2017) Synthetic RNA-Based Immunomodulatory Gene Circuits for Cancer Immunotherapy. *Cell 171*, 1138–1150.
(17) Molnár, A., Schwach, F., Studholme, D. J., Thuenemann, E. C., and Baulcombe, D. C. (2007) miRNAs control gene expression in the single-cell alga Chlamydomonas reinhardtii. *Nature 447*, 1126–1129.
(18) Zhao, T., Li, G., Mi, S., Li, S., Hannon, G. J., Wang, X.-J., and Qi, Y. (2007) A complex system of small RNAs in the unicellular green alga Chlamydomonas reinhardtii. *Genes Dev. 21*, 1190–1203.
(19) Harris, E. H. (2001) Chlamydomonas as a model organism. *Mol. Biol. 52*, 363–406.
(20) Merchant, S. S., Prochnik, S. E., Vallon, O., Harris, E. H., Karpowicz, S. J., Witman, G. B., Terry, A., Salamov, A., Fritz-Laylin, L. K., Maréchal-Drouard, L., Marshall, W. F., Qu, L. H., Nelson, D. R., Sanderfoot, A. A., Spalding, M. H., Kapitonov, V. V., Ren, Q., Ferris, P., Lindquist, E., Shapiro, H., Lucas, S. M., Grimwood, J., Schmutz, J., Grigoriev, I. V., Rokhsar, D. S., Grossman, A. R., Cardol, P., Cerutti, H., Chanfreau, G., Chen, C. L., Cognat, V., Croft, M. T., Dent, R., Dutcher, S., Fernández, E., Fukuzawa, H., González-Ballester, D., González-Halphen, D., Hallmann, A., Hanikenne, M., Hippler, M., Inwood, W., Jabbari, K., Kalanon, M., Kuras, R., Lefebvre, P. A., Lemaire, S. D., Lobanov, A. V., Lohr, M., Manuell,

A., Meier, I., Mets, L., Mittag, M., Mittelmeier, T., Moroney, J. V., Moseley, J., Napoli, C., Nedelcu, A. M., Niyogi, K., Novoselov, S. V., Paulsen, I. T., Pazour, G., Purton, S., Ral, J. P., Riaño-Pachón, D. M., Riekhof, W., Rymarquis, L., Schroda, M., Stern, D., Umen, J., Willows, R., Wilson, N., Zimmer, S. L., Allmer, J., Balk, J., Bisova, K., Chen, C. J., Elias, M., Gendler, K., Hauser, C., Lamb, M. R., Ledford, H., Long, J. C., Minagawa, J., Page, M. D., Pan, J., Pootakham, W., Roje, S., Rose, A., Stahlberg, E., Terauchi, A. M., Yang, P., Ball, S., Bowler, C., Dieckmann, C. L., Gladyshev, V. N., Green, P., Jorgensen, R., Mayfield, S., Mueller-Roeber, B., Rajamani, S., Sayre, R. T., Brokstein, P., Dubchak, I., Goodstein, D., Hornick, L., Huang, Y. W., Jhaveri, J., Luo, Y., Martínez, D., Ngau, W. C. A., Otillar, B., Poliakov, A., Porter, A., Szajkowski, L., Werner, G., and Zhou, K. (2007) The Chlamydomonas genome reveals the evolution of key animal and plant functions. *Science 318*, 245–251.

(21) Li, X., Zhang, R., Patena, W., Gang, S. S., Blum, S. R., Ivanova, N., Yue, R., Robertson, J. M., Lefebvre, P. A., Fitz-gibbon, S. T., Grossman, A. R., and Jonikas, M. C. (2016) An Indexed , Mapped Mutant Library Enables Reverse Genetics Studies of Biological Processes in Chlamydomonas reinhardtii. *Plant Cell 28*, 367–387.

(22) Scaife, M. A., Nguyen, G. T., Rico, J., Lambert, D., Helliwell, K. E., and Smith, A. G. (2015) Establishing Chlamydomonas reinhardtii as an industrial biotechnology host. *Plant J. 82*, 532–546.

(23) Shin, S.-E., Lim, J.-M., Koh, H. G., Kim, E. K., Kang, N. K., Jeon, S., Kwon, S., Shin, W.-S., Lee, B., Hwangbo, K., Kim, J., Ye, S. H., Yun, J.-Y., Seo, H., Oh, H.-M., Kim, K.-J., Kim, J.-S., Jeong, W.-J., Chang, Y. K., and Jeong, B. (2016) CRISPR/Cas9-induced knockout and knock-in mutations in Chlamydomonas reinhardtii. *Sci. Rep. 6*, 1–15.

(24) Baek, K., Kim, D. H., Jeong, J., Sim, S. J., Melis, A., Kim, J.-S., Jin, E., and Bae, S. (2016) DNA-free two-gene knockout in Chlamydomonas reinhardtii via CRISPR-Cas9 ribonucleoproteins. *Sci. Rep. 6*, 1–7.

(25) Ferenczi, A., Pyott, D. E., Xipnitou, A., and Molnar, A. (2017) Efficient targeted DNA editing and replacement in Chlamydomonas reinhardtii using Cpf1 ribonucleoproteins and single-stranded DNA. *Proc. Natl. Acad. Sci. 114*, 13567–13572.

(26) Valli, A. A., Santos, B. A. C. M., Hnatova, S., Bassett, A. R., Molnar, A., Chung, B. Y., and Baulcombe, D. C. (2016) Most microRNAs in the single-cell alga Chlamydomonas reinhardtii are produced by Dicer-like 3-mediated cleavage of introns and untranslated regions of coding RNAs. *Genome Res. 26*, 519–529.

(27) Molnar, A., Bassett, A., Thuenemann, E., Schwach, F., Karkare, S., Ossowski, S., Weigel, D., and Baulcombe, D. (2009) Highly specific gene silencing by artificial microRNAs in the unicellular alga Chlamydomonas reinhardtii. *Plant J. 58*, 165–74.

(28) Zhao, T., Wang, W., Bai, X., and Qi, Y. (2009) Gene silencing by artificial microRNAs in Chlamydomonas: TECHNICAL ADVANCE. *Plant J. 58*, 157–164.

(29) Burgess, S. J., Tredwell, G., Molnàr, A., Bundy, J. G., and Nixon, P. J. (2012) Artificial microRNA-mediated knockdown of pyruvate formate lyase (PFL1) provides evidence for an active 3-hydroxybutyrate production pathway in the green alga Chlamydomonas reinhardtii. *J. Biotechnol. 162*, 57–66.

(30) Ferrante, P., Ballottari, M., Bonente, G., Giuliano, G., and Bassi, R. (2012) LHCBM1 and LHCBM2/7 polypeptides, components of major LHCII complex, have distinct

functional roles in photosynthetic antenna system of Chlamydomonas reinhardtii. *J. Biol. Chem. 287*, 16276–16288.
(31) Wang, C., Chen, X., Li, H., Wang, J., and Hu, Z. (2017) Artificial miRNA inhibition of phosphoenolpyruvate carboxylase increases fatty acid production in a green microalga Chlamydomonas reinhardtii. *Biotechnol. Biofuels 10*, 1–11.
(32) Engler, C., Kandzia, R., and Marillonnet, S. (2008) A one pot, one step, precision cloning method with high throughput capability. *PLoS One 3*, e3647.
(33) IDT Codon Optimization Tool (https://www.idtdna.com/CodonOpt).
(34) Patron, N. J., Orzaez, D., Marillonnet, S., Warzecha, H., Matthewman, C., Youles, M., Raitskin, O., Leveau, A., Farré, G., Rogers, C., Smith, A., Hibberd, J., Webb, A. A. R., Locke, J., Schornack, S., Ajioka, J., Baulcombe, D. C., Zipfel, C., Kamoun, S., Jones, J. D. G., Kuhn, H., Robatzek, S., Van Esse, H. P., Sanders, D., Oldroyd, G., Martin, C., Field, R., O'Connor, S., Fox, S., Wulff, B., Miller, B., Breakspear, A., Radhakrishnan, G., Delaux, P. M., Loqué, D., Granell, A., Tissier, A., Shih, P., Brutnell, T. P., Quick, W. P., Rischer, H., Fraser, P. D., Aharoni, A., Raines, C., South, P. F., Ané, J. M., Hamberger, B. R., Langdale, J., Stougaard, J., Bouwmeester, H., Udvardi, M., Murray, J. A. H., Ntoukakis, V., Schäfer, P., Denby, K., Edwards, K. J., Osbourn, A., and Haseloff, J. (2015) Standards for plant synthetic biology: A common syntax for exchange of DNA parts. *New Phytol. 208*, 13–19.
(35) Crozet, P., Navarro, F., Willmund, F., Mehrshahi, P., Bakowski, K., Lauersen, K., Pérez-Pérez, M., Auroy, P., Gorchs Rovira, A., Sauret-Gueto, S., Niemeyer, J., Spaniol, B., Theis, J., Trösch, R., Westrich, L., Vavitsas, K., Baier, T., Hübner, W., de Carpentier, F., Cassarini, M., Danon, A., Henri, J., Marchand, C., de Mia, M., Sarkissian, K., Baulcombe, D., Peltier, G., Crespo, J., Kruse, O., Jensen, P., Schroda, M., Smith, A., and Lemaire, S. (2018) Birth of a photosynthetic chassis: a MoClo toolkit enabling synthetic biology in the microalga Chlamydomonas reinhardtii. *ACS Synth. Biol. 7*, 2074–2086.
(36) Stegmeier, F., Hu, G., Rickles, R. J., Hannon, G. J., and Elledge, S. J. (2005) A lentiviral microRNA-based system for single-copy polymerase II-regulated RNA interference in mammalian cells. *Proc. Natl. Acad. Sci. 102*, 13212–13217.
(37) Cai, X., Hagedorn, C. H., and Cullen, B. R. (2004) Human microRNAs are processed from capped, polyadenylated transcripts that can also function as mRNAs. *RNA 10*, 1957–1966.
(38) Lin, S. L., Chang, D., Wu, D. Y., and Ying, S. Y. (2003) A novel RNA splicing-mediated gene silencing mechanism potential for genome evolution. *Biochem. Biophys. Res. Commun. 310*, 754–760.
(39) Chung, B. Y. W., Deery, M. J., Groen, A. J., Howard, J., and Baulcombe, D. C. (2017) Endogenous miRNA in the green alga Chlamydomonas regulates gene expression through CDS-targeting. *Nat. Plants 3*, 787–794.
(40) Hu, J., Deng, X., Shao, N., Wang, G., and Huang, K. (2014) Rapid construction and screening of artificial microRNA systems in Chlamydomonas reinhardtii. *Plant J. 1*, 1052–1064.
(41) Palombella, a L., and Dutcher, S. K. (1998) Identification of the gene encoding the tryptophan synthase beta-subunit from Chlamydomonas reinhardtii. *Plant Physiol. 117*, 455–464.
(42) Szcześniak, M. W., Kabza, M., Pokrzywa, R., Gudyś, A., and Makalowska, I. (2013)

ERISdb: A database of plant splice sites and splicing signals. *Plant Cell Physiol. 54*, 1–8.
(43) Cerutti, H., Johnson, a M., Gillham, N. W., and Boynton, J. E. (1997) Epigenetic silencing of a foreign gene in nuclear transformants of Chlamydomonas. *Plant Cell 9*, 925–945.
(44) Kim, E.-J., Ma, X., and Cerutti, H. (2015) Gene silencing in microalgae: Mechanisms and biological roles. *Bioresour. Technol. 184*, 23–32.
(45) Neupert, J., Karcher, D., and Bock, R. (2009) Generation of Chlamydomonas strains that efficiently express nuclear transgenes. *Plant J. 57*, 1140–1150.
(46) Barahimipour, R., Neupert, J., and Bock, R. (2016) Efficient expression of nuclear transgenes in the green alga Chlamydomonas: synthesis of an HIV antigen and development of a new selectable marker. *Plant Mol. Biol. 90*, 403–418.
(47) Ossowski, S., Schwab, R., and Weigel, D. (2008) Gene silencing in plants using artificial microRNAs and other small RNAs. *Plant J. 53*, 674–690.
(48) Yamasaki, T., Voshall, A., Kim, E. J., Moriyama, E., Cerutti, H., and Ohama, T. (2013) Complementarity to an miRNA seed region is sufficient to induce moderate repression of a target transcript in the unicellular green alga Chlamydomonas reinhardtii. *Plant J. 76*, 1045–1056.
(49) Ebert, M. S., and Sharp, P. A. (2010) MicroRNA sponges: Progress and possibilities. *RNA 16*, 2043–2050.
(50) Reichel, M., Li, J., and Millar, A. A. (2011) Silencing the silencer: Strategies to inhibit microRNA activity. *Biotechnol. Lett. 33*, 1285–1292.
(51) Ivashuta, S., Banks, I. R., Wiggins, B. E., Zhang, Y., Ziegler, T. E., Roberts, J. K., and Heck, G. R. (2011) Regulation of gene expression in plants through miRNA inactivation. *PLoS One 6*, e21330.
(52) Liu, Q., Wang, F., and Axtell, M. J. (2014) Analysis of complementarity requirements for plant MicroRNA targeting using a Nicotiana benthamiana quantitative transient assay. *Plant Cell 26*, 741–53.
(53) Yan, J., Gu, Y., Jia, X., Kang, W., Pan, S., Tang, X., Chen, X., and Tang, G. (2012) Effective small RNA destruction by the expression of a short tandem target mimic in Arabidopsis. *Plant Cell 24*, 415–27.
(54) Mangan, S., and Alon, U. (2003) Structure and function of the feed-forward loop network motif. *Proc. Natl. Acad. Sci. U. S. A. 100*, 11980–11985.
(55) Siciliano, V., Garzilli, I., Fracassi, C., Criscuolo, S., Ventre, S., and di Bernardo, D. (2013) miRNAs confer phenotypic robustness to gene networks by suppressing biological noise. *Nat. Commun. 4*, 1–7.
(56) Bosia, C., Osella, M., Baroudi, M. El, Corà, D., and Caselle, M. (2012) Gene autoregulation via intronic microRNAs and its functions. *BMC Syst. Biol. 6*, 131.
(57) Newman, J. R. S., Ghaemmaghami, S., Ihmels, J., Breslow, D. K., Noble, M., DeRisi, J. L., and Weissman, J. S. (2006) Single-cell proteomic analysis of S. cerevisiae reveals the architecture of biological noise. *Nature 441*, 840–846.
(58) Bartel, D. P., and Chen, C.-Z. (2004) Micromanagers of gene expression: the potentially widespread influence of metazoan microRNAs. *Nat. Rev. Genet. 5*, 396–400.
(59) Murphy, K. F., Adams, R. M., Wang, X., Balázsi, G., and Collins, J. J. (2010) Tuning and controlling gene expression noise in synthetic gene networks. *Nucleic Acids Res. 38*,

2712–2726.
(60) Schmiedel, J. M., Klemm, S. L., Zheng, Y., Sahay, A., Blüthgen, N., Marks, D. S., and Oudenaarden, A. Van. (2015) MicroRNA control of protein expression noise. *Science 348*, 128–132.
(61) Stevens, D. R., Rochaix, J. D., and Purton, S. (1996) The bacterial phleomycin resistance gene ble as a dominant selectable marker in Chlamydomonas. *Mol. Gen. Genet. 251*, 23–30.
(62) Hollensen, A. K., Andersen, S., Hjorth, K., Bak, R. O., Hansen, T. B., Kjems, J., Aagaard, L., Damgaard, C. K., and Mikkelsen, J. G. (2018) Enhanced tailored microRNA sponge activity of RNA polymerase II-transcribed Tough Decoy hairpins relative to ectopically expressed ciRS7-derived circular RNAs. *Mol. Ther. - Nucleic Acids 13*, 365–375.
(63) Harris, E. (2009) Chlamydomonas in the Laboratory, in *The Chlamydomonas sourcebook* (Harris, E. H., Stern, D., and Witman, G. B., Eds.) 2nd ed., pp 241–302. Academic Press.
(64) Engler, C., Youles, M., Gruetzner, R., Ehnert, T. M., Werner, S., Jones, J. D. G., Patron, N. J., and Marillonnet, S. (2014) A Golden Gate modular cloning toolbox for plants. *ACS Synth. Biol. 3*, 839–843.
(65) Weber, E., Engler, C., Gruetzner, R., Werner, S., and Marillonnet, S. (2011) A modular cloning system for standardized assembly of multigene constructs. *PLoS One 6*, e16765.
(66) Llave, C., Xie, Z., Kasschau, K. D., and Carrington, J. C. (2002) Cleavage of Scarecrow-like mRNA targets directed by a class of Arabidopsis miRNA. *Science 297*, 2053–2056.

Figures legends

Figure 1. Construction of a synthetic circuit to measure miRNA-dependent gene repression.

A. The synthetic gene circuit to measure miRNA activity was formed by two modules: module 1, consisting of a fluorescent reporter whose expression is linked to the production of a miRNA; and module 2, comprising an mRNA of a second fluorescent reporter which carried a target site for the miRNA produced by module 1.

B. DNA constructs tested for module 1: a microRNA precursor sequence was introduced into three different sites inside a *Chlamydomonas* codon-optimized mVenus gene. The mVenus coding sequence, driven by the PSAD promoter and flanked by PSAD UTRs or PSAD 5'UTR and RBSC2 3'UTR, was split into two exons by the second intron of the *RBCS2* gene. The mVenus cassette was fused to a paromomycin-resistant cassette and transformed into the UVM11 strain.

C. Boxplot showing mVenus fluorescence measured from individual transformants carrying the constructs above. "backgr." corresponds to autofluorescence of the UVM11

strain and “neg. control” corresponds to autofluorescence of clones transformed exclusively with the paromomycin resistant cassette. On top, number of clones measured for each construct.

D. Correlation between mVenus fluorescence and intronic-encoded miRNA levels. The miRNA precursor was integrated inside the intron, at site 2. Clones expressing different levels of mVenus fluorescence were selected from panel C, and grown to exponential phase (2-3 x 10^6 cells/ml). Fluorescence was measured from the cultures (top panel), and RNA extracted for small RNA Northern blot (bottom panels). mVenus fluorescence is shown as the average of three measurements from each culture and standard deviation. U6 and miR1162 were used as loading controls.

E. Quantification of the miRNA levels from Northern Blots shown in panel D. amiRNA levels were normalized using the endogenous miRNA miR1162. Average value and standard deviation of triplicate measurements are shown.

F. Growth on TAP media containing 5-FI of clones expressing high levels of mVenus fluorescence with or without the intronic miRNA against the *MAA7* gene.

Figure 2. Construction of the miRNA-dependent repression reporter (Module 2)

A. Sites in the mCherry mRNA molecule tested for repression. The 21-nt miRNA target site of the amiRNA against *MAA7* gene was introduced into several positions of the PSAD-derived 5’ and 3’ UTRs flanking the mCherry reporter gene.

B. Measurement of mCherry fluorescence in either presence or absence of the amiRNA. One clone expressing the mCherry gene from each construct in A was re-transformed with a cassette containing the mVenus gene either with or without the intronic amiRNA against the sequenced introduced in the mCherry molecule. Only mVenus positive clones are shown. On top, number of clones analyzed in each condition. Double asterisks indicate significant differences between clones expressing the intronic miRNA and clones expressing a control construct without miRNA, for each site tested ($p<0.05$, Mann-Whitney U test).

Figure 3. Generation and characterization of synthetic miRNAs and target 3’UTR

A. Diagram of constructs used in the assay. The UVM11 strain was first transformed with the CDS of the mCherry gene flanked by PSAD-derived 5’ and 3’ UTRs. Different 21-nt sequences, with perfect complementarity to the synthetic miRNAs generated, were introduced in the 3' UTR (site C of Figure 2A). A clone with high mCherry fluorescent signal was then re-transformed with a cassette containing the mVenus gene, either with or without the corresponding intronic synthetic microRNA.

B. Boxplot of mCherry fluorescence measured from individual clones obtained as indicated in A. Only mVenus positive clones from each transformation are shown. On top, number of clones analyzed for each construct. Double asterisks indicate significant differences between clones expressing the intronic miRNA and clones expressing a control construct without miRNA ($p<0.05$, Mann-Whitney U test).

C. Synthetic miRNA sequences and levels of repression calculated from plots in B.

Figure 4. Characterization of the repressive activity of miR1

A. mCherry fluorescent signal of clones displaying increasing levels of mVenus fluorescence. “0” corresponds to autofluorescence of the UVM11 strain. mCherry-only expressing strain (no. 1) is duplicated to facilitate comparison. Average value of three measurements from same culture and standard deviation are shown.

B. mCherry fluorescence vs. mVenus fluorescence plot from clones shown in A. Black dots correspond to clones where the mVenus gene carries the intronic miRNA. White dot, clones expressing mVenus without intronic miRNA. Average value from three measurements of same culture; error bars correspond to standard deviation.

C. Northern blots showing mVenus mRNA, mCherry mRNA and miR1 miRNA levels of clones in panel A. RACK1 mRNA was used as loading control of mRNAs Northern blots, and U6 and the endogenous miR1157 as loading control of the small RNAs Northern blots.

D. Detection of miR1-dependent mCherry mRNA cleavage products. Clones expressing high levels of the mVenus gene, carrying the intronic miR1 precursor or lacking it, were subjected to modified 5’RACE. Arrowhead indicates the RT-PCR product that was recovered from the gel and sequenced.

E. Sequencing results of the RT-PCR product obtained in panel D. Arrowhead and numbers indicate the cleavage position and frequency, respectively, of the 5’ end of the truncated mCherry mRNA (top), aligned to miR1 (bottom).

F. Cells expressing mCherry only were mixed with cells expressing mCherry and mVenus. mVenus carried the intronic miR1 precursor (top panel), or lacked of intronic miRNA (bottom panel).

Figure 5. Modulation of the miRNA repressive activity

A. Plot of mCherry vs. mVenus fluorescence of independent clones. A strain expressing the mCherry gene carrying the target site for miR1 with perfect complementarity (black dots) or mismatches (white dots) was re-transformed with the mVenus cassette harboring the intronic miR1 precursor. Fluorescence of the host mCherry-expressing strain was normalized to 1. Average value and standard deviation of three measurements from same culture are shown.

B. Plot of mCherry mRNA levels against mVenus fluorescence. mCherry mRNA levels from clones in panel A were determined by RT-qPCR. Black dots represent clones expressing the mCherry gene with perfectly complementary miR1 recognition site. White dots represent clones expressing the mCherry gene with a modified (2-nt mismatch) recognition site for miR1. Average value and standard deviation of three technical replicates.

C. Northern blot to detect miR1 levels in clones expressing high levels of mVenus with the intronic miR1 precursor, or without miRNA (control). "Perfect", the mCherry gene had a miR1 target site with perfect complementarity; "mismatch", target site had a 2nt-mismatch opposite to positions 10 and 11 of the miRNA.

D. Detection of miR1-dependent mCherry mRNA cleavage products from clones in panel C. Arrowhead indicates the RT-PCR product from the 5'RACE. An endogenous miRNA target sequence, *OMT2* mRNA, was amplified as control.
E. Sequencing results of the RT-PCR product amplified in D. Arrows indicate the cleavage position and numbers indicate the frequency of these truncations.

Figure 6. De-repression of miR1 target by a miRNA decoy.
A. Constructs utilized as miRNA decoys. Target mimicry sites (marked in orange) had perfect complementarity with miR1 except for a 3-nt bulge between nucleotides opposite to positions 10 and 11 of the miRNA (see Supplementary Figure 4A). One or two target mimicry sites were incorporated into the *PSAD* 3'UTR of the mVenus gene (miRNA decoy 1X and 2X).
B. Genetic circuit to inactivate synthetic miRNA by RNA decoys. First, a strain was transformed with a mCherry cassette where mCherry mRNA carried an imperfect target site of miR1. One clone from this transformation was re-transformed with an mVenus construct carrying intronic miR1. A clone where mCherry was repressed by miR1 was finally re-transformed with an mVenus construct carrying 1 or 2 target mimicry sites in the 3'UTR. The three consecutive transformations were done using three different antibiotic selections: hygromycin, paromomycin and zeocin.
C. Boxplot showing mCherry fluorescent signals of independent clones obtained from transformation with constructs in A. All strains were compared simultaneously by the Kruskal-Wallis test of variance analysis. Double asterisks indicate significant differences with control strain expressing miRNA-repressed mCherry ($p<0.05$, pairwise Mann-Whitney U tests).

Figure 7. Construction of self-regulatory loops using intronic miRNAs.
A. Intronic miRNA self-loop (iMSL). Intron is represented in grey, and miRNA and miRNA* sequences are drawn in blue and turquoise, respectively. Splicing and processing of the miRNA precursor results in a mature miRNA that targets the mRNA that derives from the same RNA molecule as the miRNA.
B. DNA constructs to test iMSL in *Chlamydomonas*. The mVenus gene, driven by the PSAD promoter and flanked by the PSAD UTRs, was used to host the intronic miRNA precursor. Construct 1, no intronic miRNA, no target sequence; construct 2, intronic miRNA and no target site; construct 3, intronic miRNA and target site with high complementarity; construct 4, intronic miRNA and target site with internal mismatches.
C. Boxplot showing mVenus fluorescence signal of independent clones obtained from the transformations with constructs shown in B. Only mVenus positive clones are shown. "backgr." refers to autofluorescence of the UVM11 strain. On top, number of clones analyzed for each construct. All mVenus expressing strains were compared simultaneously by the Kruskal-Wallis test of variance analysis. "n.s". indicates no

significance difference; double asterisks indicate significant differences with control strains 1 and 2 ($p<0.05$, pairwise Mann-Whitney U tests).

D. Cell-to-cell variability within clones expressing different levels of the mVenus. Single-cell mVenus fluorescence was determined using flow cytometry. >8 clones stably expressing different levels of each construct indicated next to the plot were grown to early exponential phase. mVenus fluorescence from 25,000 cells from each individual clone was measured by flow cytometry. Dots in the graph correspond to each individual clone, showing average and CV^2 of the mVenus fluorescence from 25,000 cells.

Figure 1

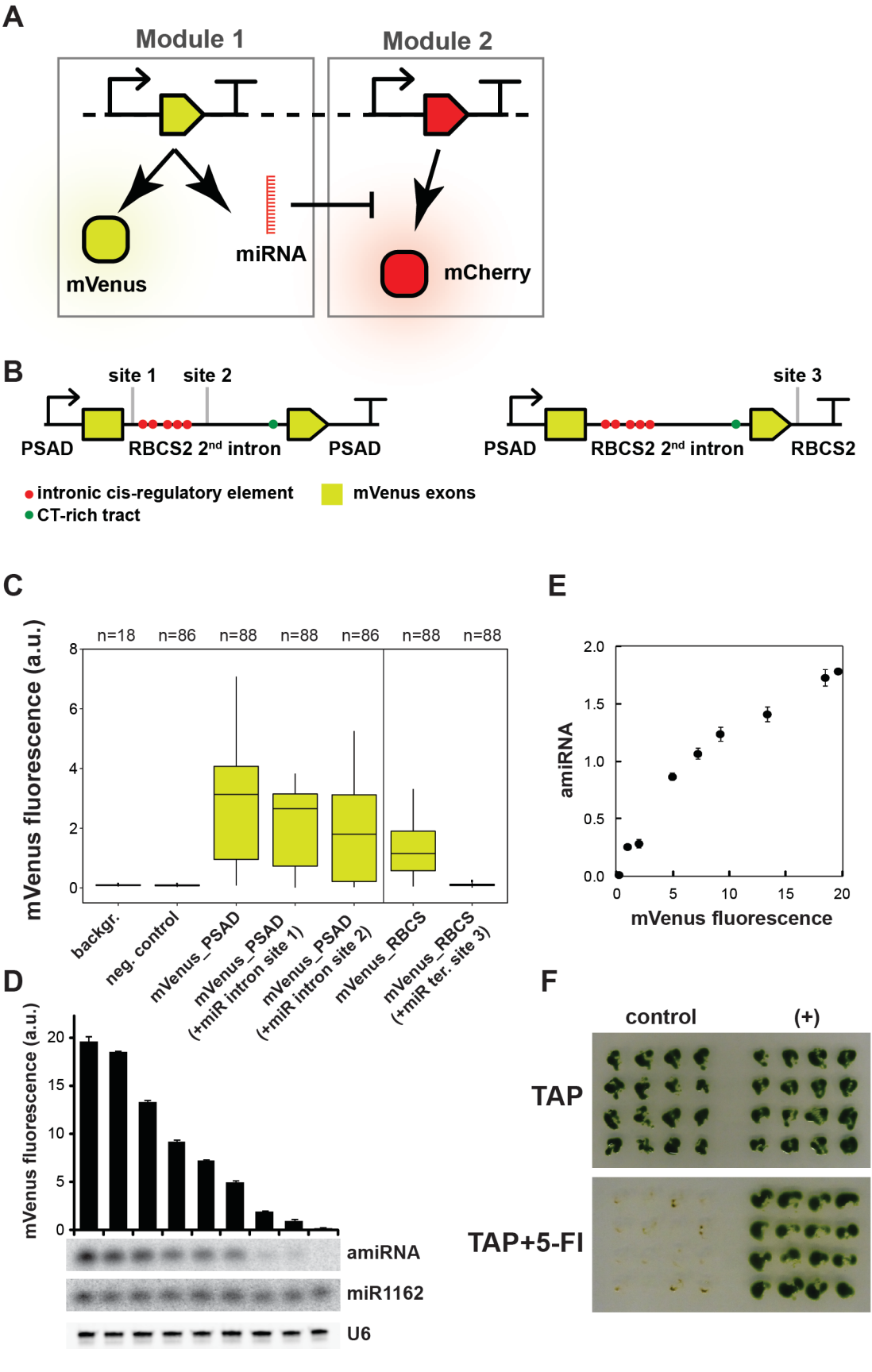
A
Module 1
Module 2
miRNA
mVenus
mCherry
B
site 1
site 2
site 3
PSAD
RBCS2 2nd intron
PSAD
PSAD
RBCS2 2nd intron
RBCS2
intronic cis-regulatory element
CT-rich tract
mVenus exons
C
mVenus fluorescence (a.u.)
n=18
n=86
n=88
n=88
n=86
n=88
n=88
backgr.
neg. control
mVenus_PSAD
mVenus_PSAD (+miR intron site 1)
mVenus_PSAD (+miR intron site 2)
mVenus_RBCS
mVenus_RBCS (+miR ter. site 3)
D
mVenus fluorescence (a.u.)
amiRNA
miR1162
U6
E
amiRNA
mVenus fluorescence
F
control
(+)
TAP
TAP+5-FI

Figure 2

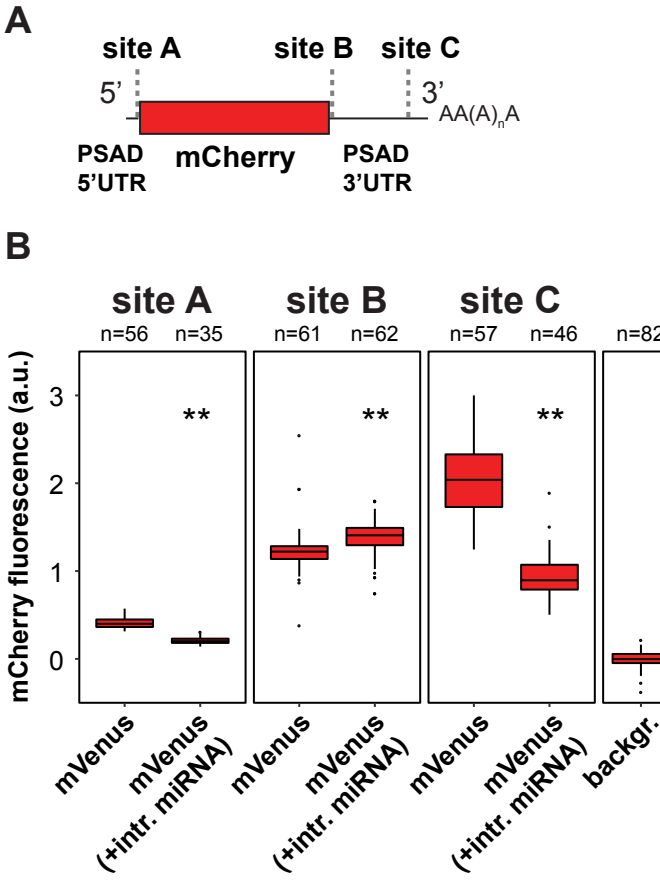
A
site A
site B
site C
5'
3'
AA(A)nA
PSAD 5'UTR
mCherry
PSAD 3'UTR
B
site A
site B
site C
n=56
n=35
n=61
n=62
n=57
n=46
n=82
mCherry fluorescence (a.u.)
0
1
2
3
**
**
**
mVenus
mVenus (+intr. miRNA)
mVenus
mVenus (+intr. miRNA)
mVenus
mVenus (+intr. miRNA)
backgr.

Figure 3

A

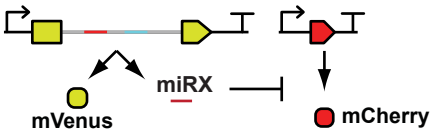

B

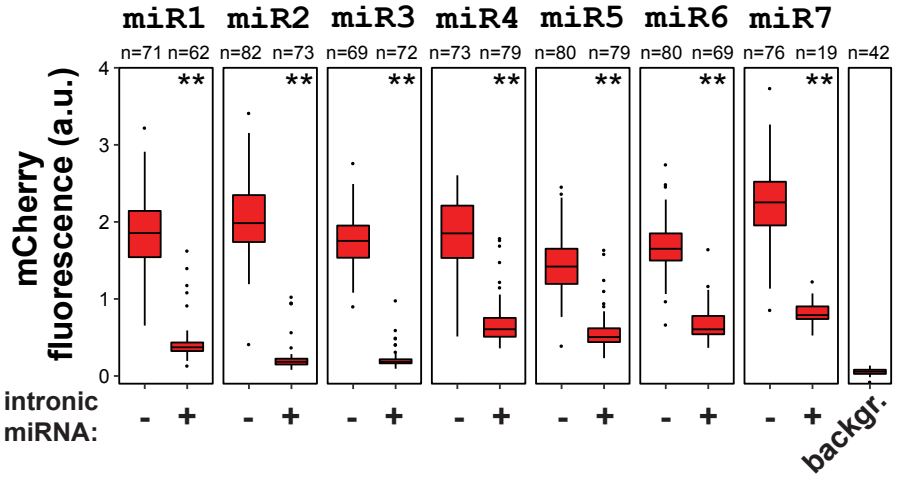

C

Name	Sequence	Repression activity
miR1	5′UAUGAAAGGCCUCUCACGCUG 3′	82%
miR2	5′UGACCGUUAUAGAAACGCCGC 3′	93%
miR3	5′UAAAGCCUAACGUUCGGCCGA 3′	93%
miR4	5′UCUAUACGUGGCAAAUCCCCC 3′	69%
miR5	5′UUUCAGCGAACGUAUACGCUC 3′	67%
miR6	5′UAUGUCUAGGCGAUCCCCCGU 3′	66%
miR7	5′UAUAUCGGGACUCGGACCCCU 3′	67%

Figure 4

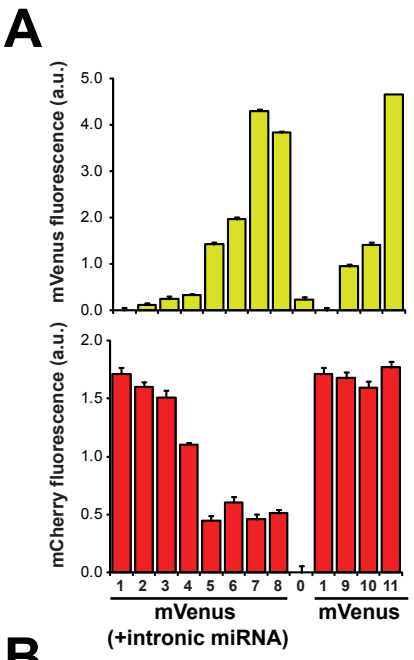
A
mVenus fluorescence (a.u.)
5.0
4.0
3.0
2.0
1.0
0.0
mCherry fluorescence (a.u.)
2.0
1.5
1.0
0.5
0.0
1 2 3 4 5 6 7 8 0 1 9 10 11
mVenus
(+intronic miRNA)
mVenus

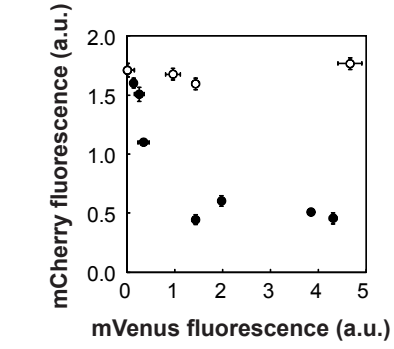
B
mCherry fluorescence (a.u.)
2.0
1.5
1.0
0.5
0.0
0 1 2 3 4 5
mVenus fluorescence (a.u.)

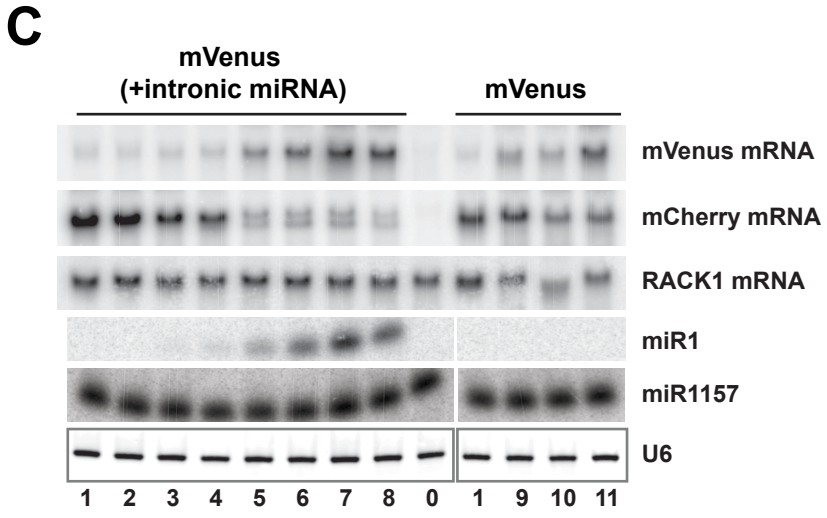
C
mVenus
(+intronic miRNA)
mVenus
mVenus mRNA
mCherry mRNA
RACK1 mRNA
miR1
miR1157
U6
1 2 3 4 5 6 7 8 0 1 9 10 11

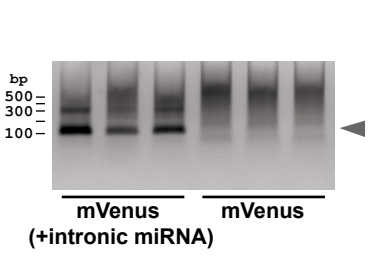
D
bp
500
300
100
mVenus
(+intronic miRNA)
mVenus

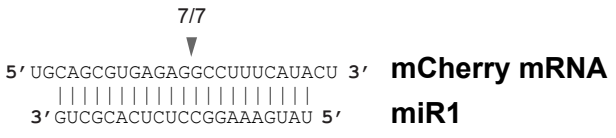
E
7/7
5′ UGCAGCGUGAGAGGCCUUUCAUACU 3′
3′ GUCGCACUCUCCGGAAAGUAU 5′
mCherry mRNA
miR1

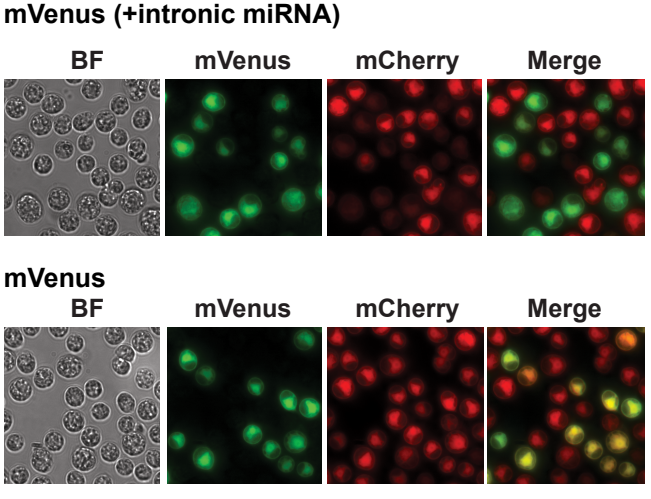
F
mVenus (+intronic miRNA)
BF
mVenus
mCherry
Merge
mVenus
BF
mVenus
mCherry
Merge

Figure 5

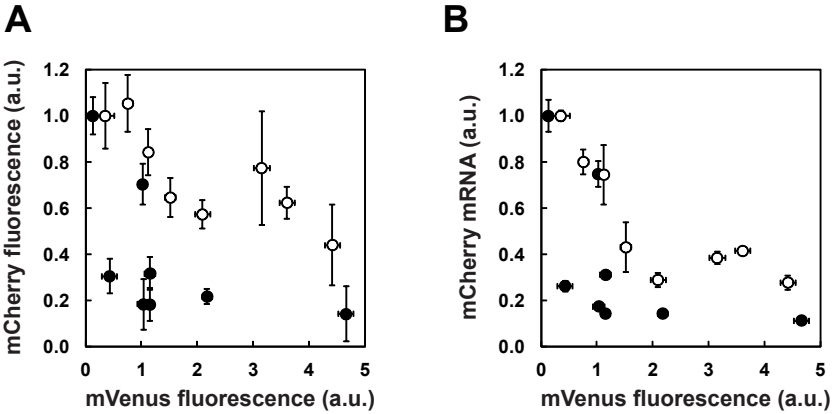
A
B
mCherry fluorescence (a.u.)
mVenus fluorescence (a.u.)
mCherry mRNA (a.u.)
mVenus fluorescence (a.u.)
0.0
0.2
0.4
0.6
0.8
1.0
1.2
0
1
2
3
4
5

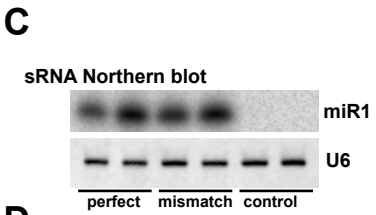
C
sRNA Northern blot
miR1
U6
perfect
mismatch
control

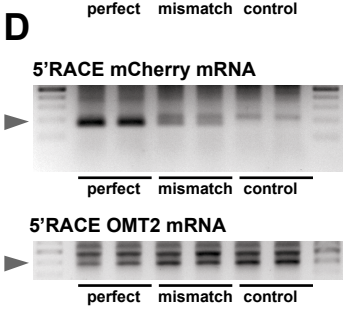
D
5'RACE mCherry mRNA
perfect
mismatch
control
5'RACE OMT2 mRNA
perfect
mismatch
control

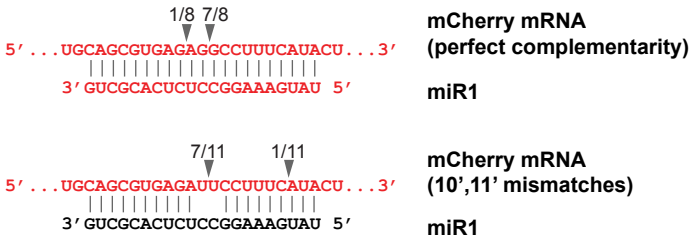
E
1/8 7/8
5'...UGCAGCGUGAGAGGCCUUUCAUACU...3'
3'GUCGCACUCUCCGGAAAGUAU 5'
mCherry mRNA
(perfect complementarity)
miR1
7/11 1/11
5'...UGCAGCGUGAGAUUCCUUUCAUACU...3'
3'GUCGCACUCUCCGGAAAGUAU 5'
mCherry mRNA
(10',11' mismatches)
miR1

Figure 6

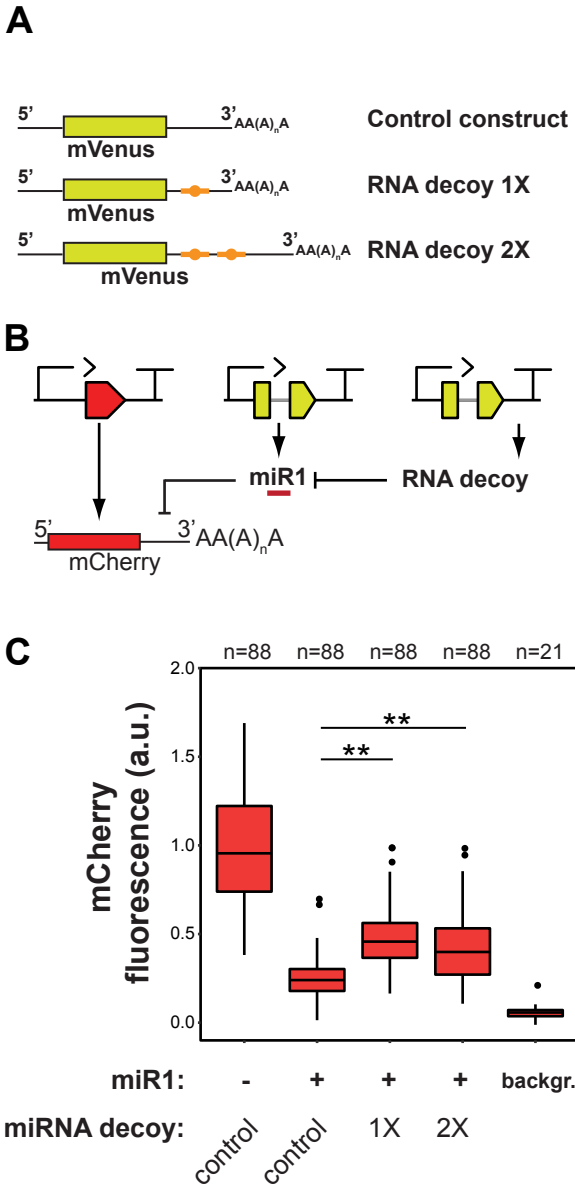
A
5'
3'AA(A)nA
mVenus
Control construct
RNA decoy 1X
RNA decoy 2X
B
miR1
RNA decoy
mCherry
C
n=88
n=88
n=88
n=88
n=21
mCherry fluorescence (a.u.)
2.0
1.5
1.0
0.5
0.0
**
**
miR1:
-
+
+
+
backgr.
miRNA decoy:
control
control
1X
2X

Figure 7

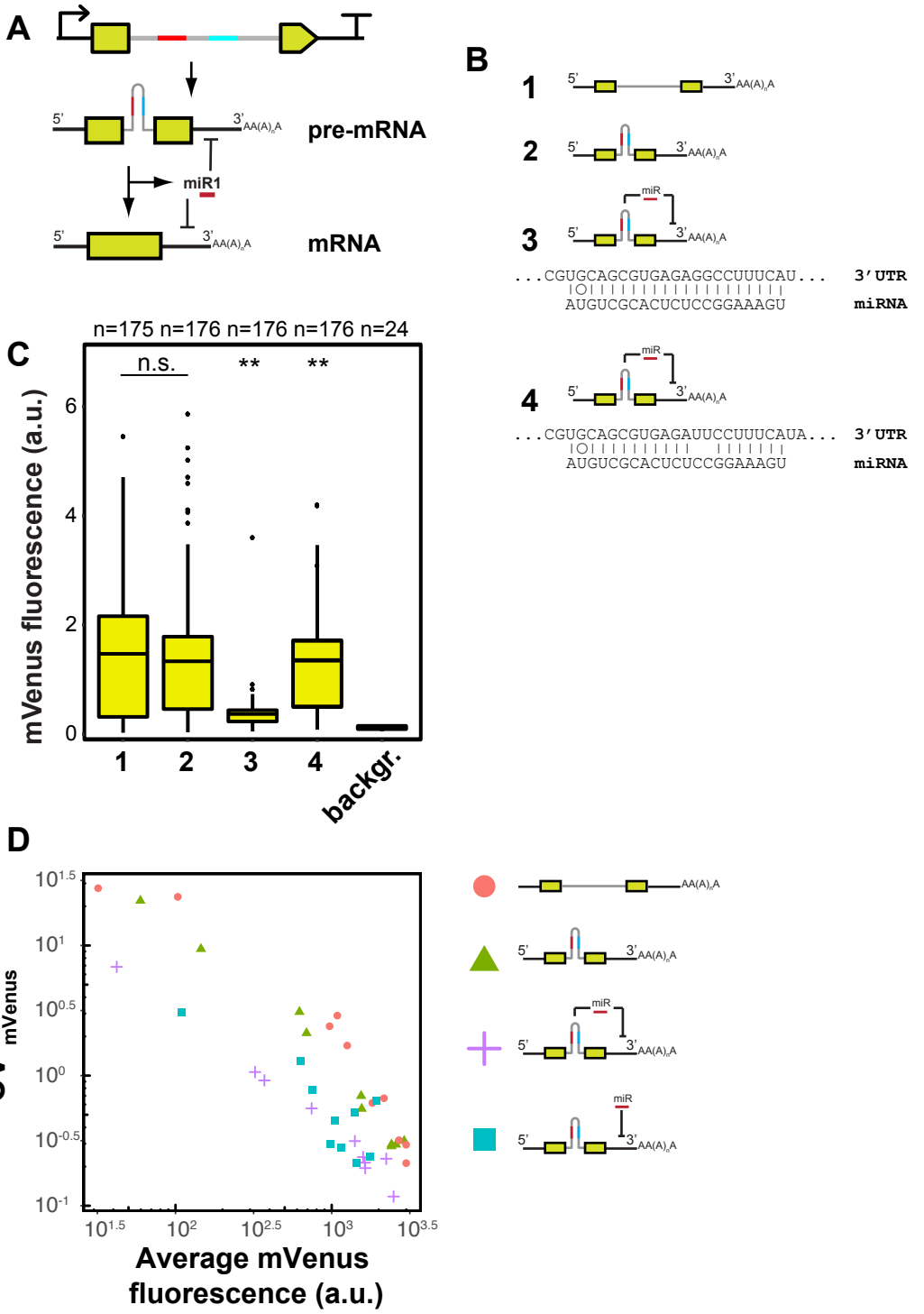
A
pre-mRNA
miR1
mRNA
B
1
2
3
...CGUGCAGCGUGAGAGGCCUUUCAU...
AUGUCGCACUCUCCGGAAAGU
3'UTR
miRNA
4
...CGUGCAGCGUGAGAUUCCUUUCAUA...
AUGUCGCACUCUCCGGAAAGU
3'UTR
miRNA
C
n=175 n=176 n=176 n=176 n=24
n.s.
**
**
mVenus fluorescence (a.u.)
backgr.
D
CV2 mVenus
Average mVenus fluorescence (a.u.)